Gain Anisotropy of the Optically Pumped Continuous Wave CF_4 Laser

M. Hartemink and H. P. Godfried

Abstract—**Gain anisotropy in an optically pumped continuous wave (CW) CF_4 laser was measured for the $P^+(31)$ emission line at 16.3 μm through a study of threshold pump powers with a continuous wave CO_2 laser, emitting at 9.3 μm. Pumping the CF_4 off line center, the gain for backward and forward traveling waves occurs at different frequencies. The frequency difference was determined using the longitudinal mode spacing of the CF_4 laser and was related to the measured pump frequency offset from absorption line center. The difference in gain between radiation emitted co-propagating and counter-propagating with the pump beam was for the first time determined quantitatively and results agreed with theoretical predictions. The occurrence of gain anisotropy is final, conclusive evidence that the lasing transition of CF_4 at 16.3 μm is directly pumped by the absorbing transition.**

Introduction

THE CF_4 laser is an example of an optically pumped three level laser where pumping and lasing transitions are coupled by a common upper level. Because of this coupling, double quantum processes (e.g., simultaneous absorption of a pump photon and emission of a 16 μm photon) occur and when at least one of the transitions involved shows some degree of Doppler broadening, these Raman processes can give rise to gain anisotropy between forward and backward emitted radiation. A theoretical description of a three level system with transitions from two of the levels to a common third level and a calculation of the resulting line shapes was already given in 1957 [1]. A more detailed and general analysis was published in 1969 [2]. This was extended to the case of high intensity pumping of one of the transitions in 1972 [3].

The semiquantum mechanical calculations are rather lengthy. However, a quick understanding of what causes the gain anisotropy may be obtained by considering the Doppler broadened line shape for the resonant Raman transition connecting the lower pump and laser levels. The Raman Doppler linewidth for the scattered wave co-propagating with the pump is much smaller than for the counter-propagating wave. Consequently the gain in the laser, being inversely proportional to the linewidth and having contributions from both the created population inversion and Raman terms, will be higher for the copropagating than for the counter-propagating wave.

Manuscript received June 17, 1991; revised August 14, 1991

The authors are with the Nederlands Centrum voor Laser Research (NCLR), 7500 CR Enschede, The Netherlands.

IEEE Log Number 9104643.

Gain anisotropy was reported in HF gas [4], optically pumped by a pulsed HF laser, by comparing the intensities in forward and backward direction. Measurements of the gain of a far-infrared laser [5] also gave a qualitative verification. But the observed anisotropy was small since the 70.5 μm emission line was optically pumped by a CO_2 laser at 9.7 μm and the theoretical gain anisotropy, given by $1 + \lambda_{gi}/\lambda_{if}$, is only of order 10%. Recently, gain anisotropy of the NH_3 laser was reported [6], [7] but again only a qualitative explanation was given. Anyway in a normal mode of operation of the NH_3 laser the two photon Raman process is used, with a large pump detuning so that only the forward wave with the highest gain occurs.

In a superfluorescence study of CF_4 using a pulse laser [8], different pulseshapes for co- and counter-propagating emitted radiation were observed in the time domain but the difference was not explained. Although experiments with an optically pumped CW CF_4 laser were reported in 1983 [9], unidirectionally pumped in a multipass cell configuration, gain anisotropy between forward and backward emitted radiation went unnoticed. In the current experiments, where the CF_4 gas was pumped off line center, co- and counter-propagating emission could be observed at different CF_4 cavity tuning settings. This enabled independent measurements of the gain in both cases and consequently of the gain anisotropy.

In the next section we first apply the results of [1]–[3] to the case of off-resonance pumping in CF_4 and the difference in gain for the two directions will be discussed. Then we will describe the experimental setup (Section III) and in Section IV we will present measurements of frequency difference, gain anisotropy ratio, and compare these data to the theory given earlier.

Theory

In many optically pumped gas lasers, the absorbing and lasing transition share a common level. In the case of the CF_4 laser (Fig. 1) the $R^+(29)\ A_1^4 + E^9 + F_1^{14}$ transition is pumped which connects the $J = 29$ rotational level of the ground state to a sublevel of the $+-$Coriolis branch of the $J = 30$ rotational state in the $(\nu_2 + \nu_4)$ combination band. Emission at frequency ν_{if} takes place from this common upper level down to the rotational level of the singly excited ν_2 vibrational state and is commonly assumed to be the $P^+(31)$ transition. In addition to the common ab-

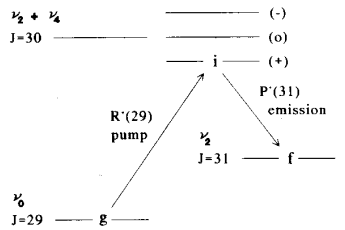

Fig. 1. Energy level configuration for the CW CF_4 laser pumped on the $R^+(29)$ $A_1^4 + E^9 + F_1^{14}$ absorption line in the $\nu_2 + \nu_4$ combination band.

sorption followed by stimulated emission transitions Raman-type transitions between the ground state and ν_2 level can take place. For a $S_1(29)$ transition this results in a scattered photon whose frequency is within the gain bandwidth of the CF_4 laser.

For a theoretical description of this three level system, we follow the model given by [2] and which was also used by Seligson *et al.* [5]. We designate ground, intermediate, and final levels of the three level system with symbols g, i, and f, respectively. The pump transition with center frequency $\nu_{gi,0}$ is pumped at frequency ν_{gi}, emission takes place at frequency ν_{if}. Emission line center is at frequency $\nu_{if,0}$. In the model the pump field E_{gi} can be of arbitrary strength but the emitted field E_{if} is assumed to be weak. Relaxation rates for population decay (γ_g, γ_i, γ_f), polarization decay (γ_{gi}, γ_{if}), and Raman coherence decay (γ_{gf}) are all included in the theory, with the subscripts indicating the levels involved. Another important quantity is the normalized velocity distribution function $W(v)$, with v the velocity component in the propagation direction of the pump field:

$$W(v) = \sqrt{\frac{M}{2\pi kT}} \exp\left(-\frac{Mv^2}{2kT}\right).$$

This is the usual distribution for molecules of mass M at a temperature T, with k the Boltzmann constant. With the assumption that in the absence of the pump field all molecules are in the ground state, and in the presence of a pump field E_{gi} at frequency ν_{gi}, the gain at the emission frequency ν_{if} is given by [5]

$$G(\nu_{if}) = G_0 \beta^2 \operatorname{Im} \gamma_{if} \int \frac{L_{gi} - 2R\dfrac{\gamma_{gi}}{\gamma_i}}{AB} W(v)\, dv \quad (1)$$

where

$$G_0 = \frac{8\pi^2 \nu_{if,0}}{c} \frac{\mu_{if}^2}{\hbar} \frac{N}{\gamma_{if}}$$

$$\beta = \frac{\mu_{gi} E_{gi}}{2\hbar}$$

$$R = (\Delta'_{if} - \Delta'_{gi}) - i\gamma_{gf}$$

$$A = |L_{gi}|^2 + 4\beta^2 \gamma_{gi}^2 / \gamma_i \gamma_g$$

$$B = -RL_{if}^* + \beta^2$$

$$L_{if} = \Delta'_{if} + i\gamma_{if}$$

$$L_{gi} = -\Delta'_{gi} + i\gamma_{gi}$$

$$\Delta'_{if} = 2\pi\left(\nu_{if}\left(1 - \frac{v}{c}\right) - \nu_{if,0}\right)$$

$$\Delta'_{gi} = 2\pi\left(\nu_{gi}\left(1 - \epsilon\frac{v}{c}\right) - \nu_{gi,0}\right).$$

The parameter ϵ is $+1(-1)$ for emitted photons co-propagating (counter-propagating) with the incident pump photons and μ is the transition dipole moment. The general expression (1) can be used to obtain the more specific expressions (cf. [5]) for homogeneously broadened systems, systems in which only the pump transition is Doppler broadened or fully Doppler broadened systems.

When both transitions are Doppler broadened, as in our experiment, there will be a directional anisotropy in the gain. If population decay is collision dominated and dephasing collisions can be ignored we can simplify the equations by assuming all relaxation rates to be equal ($\gamma = \gamma_g = \gamma_i = \gamma_f$). For a weak pump intensity (1) can be integrated to give a resulting Lorentzian emission line shape. The total area under the two Lorentzians is equal for the propagation directions, but the linewidth in the forward direction ($\epsilon = +1$) is narrower than in the backward direction ($\epsilon = -1$). The FWHM linewidths are given by

$$\gamma(\epsilon) = 2\gamma + (1 - \epsilon)\,\gamma \frac{\nu_{if,0}}{\nu_{gi,0}}. \quad (2)$$

A direct consequence of (2) is a directional gain anisotropy with higher gain in the forward direction.

Equations (1) and (2) may be used to calculate the gain and output power of the CF_4 laser. In the absence of a pump field the ground state population is N_g and the Doppler width for absorption is $\Delta\nu_{D,gi}$. The gain $G(\epsilon)$ induced by a pump field E_{gi} with a frequency shifted by $\Delta\nu_{gi} (= \nu_{gi} - \nu_{gi,0})$ from absorption line center is given by

$$G(\epsilon) = \sqrt{\frac{\ln 2}{\pi}} \frac{8\pi^2 \nu_{if,0}}{c} \frac{\mu_{if}^2}{\hbar} N_g \cdot \frac{\exp\left(-4 \ln 2 \left(\dfrac{\Delta\nu_{gi}}{\Delta\nu_{D,gi}}\right)^2\right)}{\Delta\nu_{D,gi}} \cdot \left(\frac{\mu_{gi} E_{gi}}{2\hbar}\right)^2 \frac{1}{\gamma\gamma(\epsilon)}. \quad (3)$$

It is clear that the gain depends linearly on the pump power P_{gi} (no saturation) and inversely on the linewidth $\gamma(\epsilon)$

$$G(\epsilon) \sim \frac{P_{gi}}{\gamma(\epsilon)}. \quad (4)$$

For a laser with gain length L, interaction cross section A, and losses t due to output coupling, the output power

P_{if} of the laser is given by [10]

$$P_{if} = \frac{1}{2} I_{\text{sat}} tA \left\{ \frac{2LG(\epsilon)}{\alpha(p, T) + t} - 1 \right\} \tag{5}$$

where I_{sat} is the saturation intensity for the lasing transition and $\alpha(p, T)$ the intracavity losses. This expression is valid only when the losses α and t are small compared to unity, as is the case in our system.

To calculate the output power of the laser it is important to realize that the saturation intensity I_{sat} strongly depends on the timescale for which the output is studied. For the CW laser the saturation intensity is determined by diffusion time of excited molecules to the walls which takes place on a ms-timescale for the pressure and temperature range studied. In a CF_4 laser pumped by a pulsed CO_2 laser (e.g., a TEA laser) the saturation intensity is determined by the rotational relaxation resulting in high values of I_{sat}. In this paper we will focus on the pump threshold and we are therefore only concerned with the expression in brackets. It should be noted that the intracavity losses $\alpha(p, T)$ appearing in that expression include absorption losses because of the thermally populated lower laser level. At a fixed pressure and temperature these losses are constant and the threshold condition is given by

$$G(\epsilon) = \frac{\alpha(p, T) + t}{2L} = \text{cst.} \tag{6}$$

Determining the threshold pump power for both forward and backward traveling waves, we get [combining (4) and (6)]

$$\frac{P_{\text{thr}}(\epsilon = +1)}{P_{\text{thr}}(\epsilon = -1)} = \frac{\gamma(\epsilon = +1)}{\gamma(\epsilon = -1)}. \tag{7}$$

The threshold pump power for the radiation traveling in opposite directions can easily be determined in a ring laser configuration where the two components are spatially separated. In a standing wave system this can also be achieved by off-resonance pumping if the longitudinal mode spacing of the cavity is larger than the Doppler linewidth. In off-resonance pumped Doppler broadened systems using a narrow-band pump laser results in velocity selective excitation of molecules with frequencies Doppler shifted to match the pump laser frequency. Emission may take place in both the forward and backward direction. The shift from resonance of the pump determines the velocity of the excited molecules and thereby also the Doppler shift $\Delta\nu_{if}$ for emission

$$\left| \frac{\Delta\nu_{gi}}{\nu_{gi,0}} \right| = \left| \frac{\Delta\nu_{if}}{\nu_{if,0}} \right| = \frac{v}{c}. \tag{8}$$

Consequently, the difference between the frequencies of the copropagating wave ν^+ and counter-propagating wave ν^- is given by

$$\nu^+ - \nu^- = 2 \cdot \left[\frac{\Delta\nu_{gi}}{\nu_{gi,0}} \right] \cdot \nu_{if,0}. \tag{9}$$

When the homogeneous linewidth and the frequency difference $(\nu^+ - \nu^-)$ are much smaller than the longitudinal mode spacing of the laser, it is possible to study the gain for co- and counter-propagating waves by tuning the cavity length in resonance with either of these waves.

Experimental Setup

A schematic of the experimental setup is shown in Fig. 2. A sealed-off CW CO_2 laser, tuned to the 9R(12) emission line, was used to pump the CF_4. The CO_2 laser cavity was formed by an 80% reflectivity concave mirror, with a radius of curvature of 3 m and a grating (150 L/mm) mounted in a littrow configuration to line tune the laser. The grating was mounted on a piezo transducer to allow length tuning of the CO_2 laser. An optoacoustic cell was used to lock the CO_2 laser to the CF_4 absorption line which is shifted 31 MHz to the blue side of the 9R(12) line center [11]. We could also sweep the frequency with the piezo to tune the laser through the absorption maximum. Frequency was calibrated against the drive voltage using the longitudinal mode spacing ($c/2l$ = 95 MHz) of the CO_2 laser. Nonlinearities in the piezo gave errors of less than 5% in the frequency determination.

The 278 cm long CF_4 laser cavity consisted of two dichroic mirrors, with an 98% reflectivity at 16 μm while transmitting 80% of the pump radiation. Their radius of curvature was 3 m. The CF_4 cavity was stabilized with Invar bars and could be tuned piezoelectrically. We note that the longitudinal mode spacing ($c/2l$ = 54 MHz) is much larger than the velocity selected homogeneous emission linewidth ($\approx$ 1 MHz).

The pump beam was mode matched to the 16 μm cavity using two lenses. It should be noted that plane parallel plates [12] and the two KBr prisms introduced astigmatism in the pump beam which easily amounted to differences of 10% in the beam waist size in horizontal and vertical direction so that, without compensation, the pump beam shape is always a compromise. Pump beam and generated output beam were aligned to travel collinearly to maximize conversion efficiency. KBr prisms were needed to separate pump and output beams. In this configuration, reflections from the mirrors back to the pump laser seriously degraded the stability of the pump laser frequency. To overcome this problem a $\lambda/4$ plate in conjunction with two Ge Brewster plates was used to minimize optical feedback. The $\lambda/4$ plate not only ensured a stable pump laser frequency but is also predicted to increase the small-signal gain of the laser by a factor of 1.5 [13].

The CF_4 laser chamber could be cooled with cold nitrogen gas. Both ends of the cell were kept at room temperature, the cooled section was approximately 210 cm long. Temperatures were monitored using 3 Pt resistors near the wall of the cell. They showed a residual temperature difference of approximately 20 K along the cells cold section.

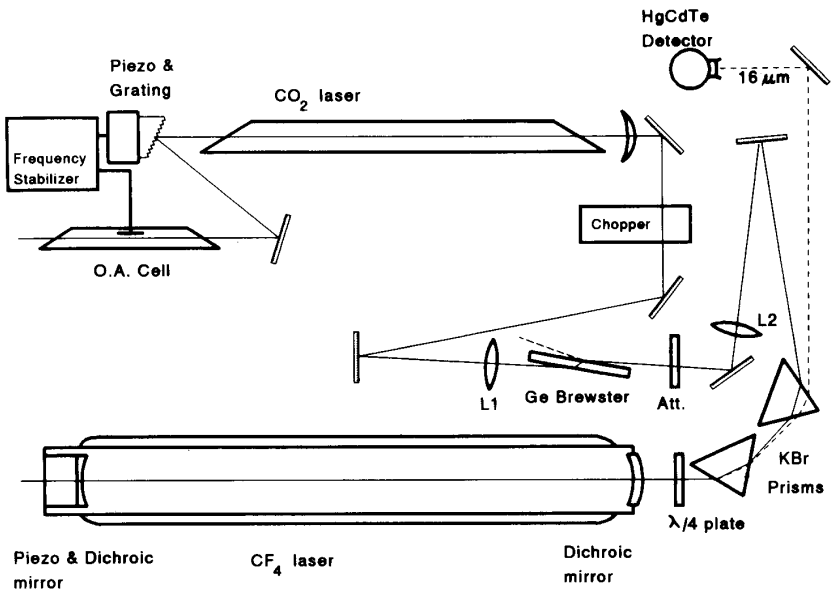

Fig. 2. Experimental setup.

The 16 μm radiation was monitored with a HgCdTe detector. Light levels were adjusted using a silicon absorption filter to avoid saturation of the detector and clipping of the amplifier. The CO_2 laser pump power was monitored in the beam behind lens *L2* with a power meter which was removed during output power measurements of the CF_4 laser. A plane parallel Ge or ZnSe plate was used to vary the pump power. The plate, which acted as a Fabry–Perot, could be rotated. In the case of ZnSe a maximum of 50% attenuation was obtained while for Ge maximum attenuation was 75%.

Results

First, we determined the pump-offset from absorption line center. In a previous experiment the frequency shift of the CF_4 absorption line center to the CO_2 emission linecenter was found to be 31 MHz [11]. Calculations on the basis of the emission linewidth of the CO_2 laser and the absorption linewidth of the CF_4 gas in the optoacoustic cell, multiplying pump power and absorption, show that maximum power deposition occurs at 25 MHz from CO_2 emission line center. The underlying assumption of the multiplication is that absorption in the optoacoustic cell α is small compared to unity. Using the CO_2 laser longitudinal mode spacing to calibrate the frequency shift we found that maximum optoacoustic signal occurred 26 $\pm$ 1 MHz from CO_2 emission line center. Consequently the pump-offset is given by $\Delta\nu_{gi} = 5$ MHz.

When slowly scanning the CF_4 cavity length we observe output peaks as shown in Fig. 3. The repetition of the pattern reflects the 16 μm cavity longitudinal mode spacing while the smaller and larger peaks are associated

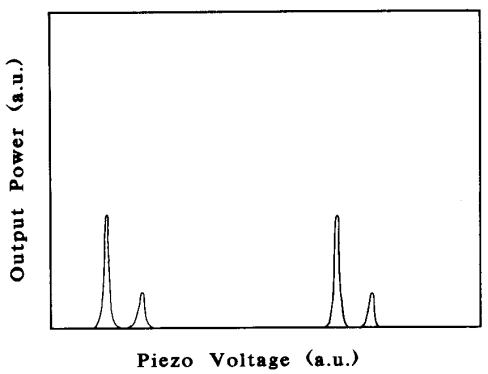

Fig. 3. CF_4 output as a function of piezo drive voltage.

with backward and forward emitted radiation. If we use the CF_4 cavity longitudinal mode spacing to calibrate the frequency we get for the frequency difference between co-propagating and counter-propagating waves:

$$\nu^+ - \nu^- = 6 \pm 1 \text{ MHz}.$$

In view of (8) this value is in good agreement with the measured pump-offset. The width of the output peaks were of the order of 1 MHz. The current agreement between these measurements provides an independent confirmation for the value of the shift between CF_4 absorption linecenter and CO_2 emission line center reported earlier [11].

Both for the higher peaks (forward emission) and the smaller output peaks (backward emission) we measured the CW 16 μm output as a function of CO_2 pump power. The output showed the expected linear dependence on the

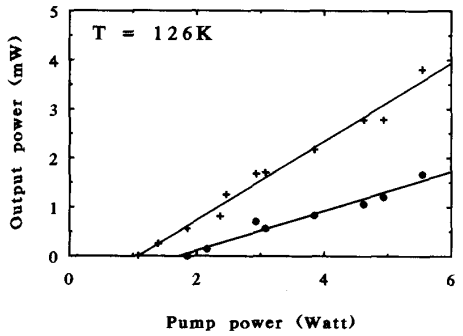

Fig. 4. Output power of the CF_4 laser as a function of pump power at a pressure of 4.0 Pa and at a temperature of 126 K. Indicated are measurements for forward (+) and backward (●) emitted radiation.

pump power [10]. Also no splitting was observed, indicating the absence of ac stark splitting at these power levels. We measured the pump power dependence of the output at pressures of 4.0 Pa and 6.7 Pa, at different temperatures. As an example, the results are shown for a pressure of 4.0 Pa at 126 K (Fig. 4). The quality of the data and of the fits at other temperatures and pressures is very similar. The data were fitted using a least squares method and the threshold pump powers determined (Table I). We see that threshold pump powers increase as a function of pressure and temperature. These dependencies will be discussed in a separate publication [14].

Averaging the threshold pump power ratio's given in Table I we conclude that the threshold pump power ratio for forward P^+_{thr} and backward traveling radiation P^-_{thr} is given by

$$R = \frac{P^-_{thr}}{P^+_{thr}} = 1.5 \pm 0.1.$$

As discussed earlier the pump threshold ratio for co-propagating and counter-propagating waves equals the linewidth ratio which according to theoretical predictions is $R = 1 + \nu_{if,0}/\nu_{gi,0} = 1.57$. This theoretical value is confirmed within error by our measurements of the threshold pump powers.

Although strong indications were found earlier [15] that the emitting transition in CF_4 is the $P^+(31)$ transition, the current experiment, in which the occurrence of gain anisotropy was demonstrated and the theoretical predictions were quantitatively confirmed, provides final, conclusive evidence that this transition is indeed involved. For any other transition where gain is obtained via indirect pumping of the laser upper level the absence of Raman terms would imply the absence of gain anisotropy.

With this result we have shown that the theory given by Feld and Javan [2] not only gives a qualitative but also an accurate quantitative prediction of the gain anisotropy effect. It is important to realize that the linewidth differences between backward and forward emitted radiation will remain even when the absorbing transition is pumped on-resonance. Consequently, the total gain will then be the addition of the gain in the forward and backward direction [3] in sharp contrast to rate equations model predictions. In all optically pumped lasers with a common upper level double quantum transitions play an important role. Only in the limiting case that $\nu_{if}/\nu_{gi} \rightarrow 0$ the gain ratio $R \rightarrow 1$ and the laser can be described by a rate equations model. In all other cases Raman effects on linewidth and line shape have to be taken into account.

TABLE I
THRESHOLD PUMP POWERS FOR FORWARD AND BACKWARD EMITTED RADIATION

Pressure p(Pa)	Temp. T(K)	Pump Threshold P^+_{thr}(W)	Pump Threshold P^-_{thr}(W)	Ratio R
4.0	142	1.12 ± 0.13	1.80 ± 0.11	1.6 ± 0.3
4.0	126	1.08 ± 0.11	1.70 ± 0.18	1.6 ± 0.3
4.0	113	0.86 ± 0.08	1.12 ± 0.31	1.3 ± 0.5
6.7	142	1.83 ± 0.09	2.63 ± 0.31	1.4 ± 0.2
6.7	126	1.62 ± 0.16	2.37 ± 0.21	1.5 ± 0.3
6.7	113	1.00 ± 0.09	1.53 ± 0.16	1.5 ± 0.3

SUMMARY

We have shown that gain anisotropy in optically pumped lasers for forward and backward emitted radiation can be determined by pump threshold measurements. For the first time the ratio of forward and backward gain, the gain anisotropy ratio, R has been measured. For the CW CF_4 laser we measured $R = 1.5 \pm 0.1$ which agrees within error with the theoretical prediction $R = 1.57$. The demonstration of gain anisotropy in the CF_4 laser provides conclusive evidence that the lasing transition is directly pumped by the absorbing transition.

REFERENCES

[1] A. Javan, "Theory of a three-level maser," *Phys. Rev.*, vol. 107, pp. 1579-1589, 1957.
[2] M. S. Feld and A. Javan, "Laser-induced line-narrowing effects in coupled Doppler-broadened transitions," *Phys. Rev.*, vol. 177, pp. 540-562, 1969.
[3] B. J. Feldman and M. S. Feld, "Laser-induced line-narrowing effects in coupled Doppler-broadened transitions. II. Standing-wave features," *Phys. Rev.*, vol. A5, pp. 899-918, 1972.
[4] N. Skribanowitz, I. P. Herman, R. M. Osgood, M. S. Feld, and A. Javan, "Anisotropic ultrahigh gain emission observed in rotational transitions in optically pumped HF gas," *Appl. Phys. Lett.*, vol. 20, pp. 428-431, 1972.
[5] D. Seligson, M. Ducloy, J. R. R. Leite, A. Sanchez, and M. S. Feld, "Quantum mechanical features of optically pumped CW FIR lasers," *IEEE J. Quantum Electron.*, vol. QE-13, pp. 468-472, 1977.
[6] P. Wazen and G. L. Bourdet, "Experimental investigation of the MIR optically pumped ammonia bidirectional ring laser," *Appl. Phys.*, vol. B49, pp. 377-381, 1989.

[7] ——, "Gain anisotropy and simultaneous bidirectional emission of Doppler-broadened MIR optically-pumped ammonia ring-laser," *IEEE J. Quantum Electron.*, vol. 27, pp. 152–157, 1991.
[8] J. M. Green, T. Stamatakis, and J. D. Aldcroft, "Characteristics of the 615 cm^{-1} superfluorescent emission from CO_2 laser-pumped CF_4," *Opt. Commun.*, vol. 39, pp. 99–104, 1981.
[9] J. Telle, "Continuous wave CF_4 laser," *IEEE J. Quantum Electron.*, vol. QE-19, pp. 1469–1473, 1983.
[10] A. Siegman, *Lasers*. Mill Valley, CA: Univ. Sci. Books, 1986.
[11] M. Hartemink and H. P. Godfried, "CF_4 combination band absorption spectroscopy," *J. Mol. Spectrosc.*, vol. 148, pp. 1–12, 1991. The value of 34 MHz for the shift of the absorption from CO_2 line center has to be corrected for mode-pulling effects in the CO_2 laser which amounted to approximately 8% in our system. See also [10], pp. 466–473.
[12] H. W. Kogelnik, E. P. Ippen, A. Dienes, and C. V. Shank, "Astigmatically compensated cavities for cw dye lasers," *IEEE J. Quantum Electron.*, vol. QE-8, pp. 373–379, 1972.
[13] S. J. Petuchowski and T. A. DeTemple, "Optimum emission polarization and power enhancement in circularly polarized optically pumped lasers," *Opt. Lett.*, vol. 6, pp. 227–229, 1981.
[14] M. Hartemink and H. P. Godfried, "A parametric study of the output of the optically pumped CW CF_4 laser," *IEEE J. Quantum Electron.*, to be published.
[15] R. S. McDowell, C. W. Patterson, C. R. Jones, M. I. Buchwald, and J. M. Telle, "Spectroscopy of the CF_4 laser," *Opt. Lett.*, vol. 4, pp. 274–276, 1979.

M. Hartemink, photograph and biography not available at the time of publication.

H. P. Godfried, photograph and biography not available at the time of publication.